

1 **Running head:** ???

2 Cranial morphological disparity within the  
3 adaptive radiation of tenrecs (Afrosoricida,  
4 Tenrecidae) is no greater than expected by  
5 chance

6 Sive Finlay<sup>1,2,\*</sup> and Natalie Cooper<sup>1,2</sup>

7 <sup>1</sup> School of Natural Sciences, Trinity College Dublin, Dublin 2, Ireland.

8 <sup>2</sup> Trinity Centre for Biodiversity Research, Trinity College Dublin, Dublin 2, Ireland.

9 \*sfinlay@tcd.ie; Zoology Building, Trinity College Dublin, Dublin 2, Ireland.

10 Fax: +353 1 6778094; Tel: +353 1 896 2571.

11 **Keywords:** disparity, morphology, geometric morphometrics, tenrecs,  
12 golden moles adaptive radiation

## <sup>13</sup> **Abstract**

## 14 Introduction

15 Adaptive radiations, "evolutionary divergence of members of a single  
16 phylogenetic lineage into a variety of different adaptive forms" (Futuyma  
17 1998, cited by Losos, 2010) have long-attracted the interests and attentions  
18 of naturalists. Some of the most famous examples include Darwin's  
19 finches, cichlid fish and Caribbean *Anolis* lizards (Gavrillets & Losos, 2009).  
20 These groups exhibit great variety in both species richness and  
21 phenotypic diversity. However, taxonomic diversity does not necessarily  
22 correlate with phenotypic variety (Ruta et al., 2013; Hopkins, 2013) and  
23 clades that have exceptional phenotypic diversity can still be regarded as  
24 adaptive radiations even if they are not taxonomically diverse. Therefore,  
25 to determine whether a clade has adaptively radiated it is important to  
26 test whether it exhibits exceptional (i.e. greater than expected by chance)  
27 morphological and ecological diversity (Losos & Mahler, 2010). However,  
28 few adaptive radiations have been characterised in this way.

29 Phenotypic diversity is commonly measured as morphological  
30 disparity; the diversity of organic form (Foote, 1997; Erwin, 2007)). There  
31 is no single definition of disparity and it can be calculated in many ways  
32 including measures of morphospace occupation (e.g. Goswami et al., 2011;  
33 Brusatte et al., 2008) and rate-based approaches that assess the amount of  
34 directed change away from an ancestor (O'Meara et al., 2006; Price et al.,  
35 2013). Analyses of disparity apply these alternative approaches depending  
36 on whether the study is interested in current patterns of morphological  
37 diversity or the rate at which they accumulate through time.

38 Here we investigate current patterns of morphological disparity in  
39 tenrecs (Afrosoricida, Tenrecidae) to determine whether they represent an

40 adaptive radiation sensu (Losos & Mahler, 2010). The tenrec family is  
41 comprised of 34 species, 31 of which are endemic to Madagascar (Olson,  
42 2013). From a single common ancestor (Asher & Hofreiter, 2006),  
43 Malagasy tenrecs diversified into a wide variety of descendant species  
44 which convergently resemble distantly related insectivore mammals such  
45 as shrews (*Microgale* tenrecs), moles (*Oryzorictes* tenrecs) and hedgehogs  
46 (*Echinops*, *Setifer* tenrecs) (Eisenberg & Gould, 1969).

47 Tenrecs are often cited as an example of an adaptively radiated family  
48 which exhibits exceptional morphological diversity (Soarimalala &  
49 Goodman, 2011; Olson & Goodman, 2003; Eisenberg & Gould, 1969).  
50 However, this apparent exceptional diversity is based on subjective  
51 comparisons to other groups and it has not been tested quantitatively. If  
52 tenrecs are exceptionally morphologically diverse then there are two  
53 predictions; tenrecs are more morphologically disparate than expected by  
54 chance and they are significantly more diverse than their nearest relatives,  
55 the golden moles (Afrosoricida, Chrysochloridae).

56 Using the most complete morphological data set of tenrecs and golden  
57 moles to date we apply geometric morphometric analyses (Rohlf &  
58 Marcus, 1993; Zelditch et al., 2012) to quantify morphological disparity  
59 among our species. Our results indicate that, on average, tenrecs are more  
60 phenotypically diverse than their closest relatives but their morphological  
61 diversity is no greater than that which is expected to evolve by chance.  
62 Therefore, under strict definitions, their designation as an exceptional  
63 adaptive radiation may need to be reconsidered.

64 These findings highlight the vital importance of testing our common,  
65 but often erroneous, expectations about patterns of morphological

66 disparity in groups that exhibit apparent high levels of diversity.

## 67 **Materials and Methods**

### 68 **Data collection**

#### 69 **Morphological data collection**

70 One of us (SF) photographed cranial specimens of tenrecs and golden  
71 moles at the Natural History Museum London (NHML), the Smithsonian  
72 Institute Natural History Museum (SI), the American Museum of Natural  
73 History (AMNH), Harvard's Museum of Comparative Zoology (MCZ)  
74 and the Field Museum of Natural History, Chicago (FMNH). We  
75 photographed the specimens with a Canon EOS 650D camera fitted with  
76 an EF 100mm f/2.8 Macro USM lens using a standardised procedure to  
77 minimise potential error (see supplementary material for details).

78 We collected pictures of the skulls in dorsal, ventral and lateral views  
79 (right side of the skull) and of the outer (buccal) side of the right  
80 mandibles. A full list of museum accession numbers and access to the  
81 images can be found in the supplementary material.

82 In total we collected pictures from 182 skulls in dorsal view (148  
83 tenrecs and 34 golden moles) and 181 mandibles in lateral view (147  
84 tenrecs and 34 golden moles), representing 31 species of tenrec (out of the  
85 total 34 in the family) and 12 species of golden moles (out of a total of 21  
86 in the family (Asher et al., 2010)). We used the taxonomy of Wilson and  
87 Reeder (2005) supplemented with more recent sources (IUCN, 2012;  
88 Olson, 2013) to identify our specimens.

89 We used a combination of both landmarks (type 2 and type 3,  
90 (Zelditch et al., 2012)) and semilandmarks to characterise the shapes of  
91 our specimens. Our landmarks (points) and semilandmarks (outline  
92 curves) used to represent shape variation in the dorsal skulls and  
93 mandibles are depicted in Figures 1 and 2 respectively. Corresponding  
94 landmark definitions for each view are in tables 1 and 2. We also placed  
95 landmarks and semilandmarks on photographs of ventral and lateral skull  
96 views, details can be found in the supplementary material. We digitised  
97 all landmarks and semilandmarks in tpsDIG, version 2.17 (Rohlf, 2013).

98 We re-sampled the outlines to the minimum number of evenly spaced  
99 points required to represent each outline accurately (MacLeod, 2013,  
100 details in supplementary material). We used TPSUtil (Rohlf, 2012) to  
101 create sliders files (Zelditch et al., 2012) to define which points were  
102 semilandmarks. We conducted all subsequent analyses in R version 3.0.2  
103 (R Development Core Team, 2013) within the geomorph package (Adams  
104 et al., 2013). We used the gpagen function to run a general Procrustes  
105 alignment (REFS) of the landmark coordinates while sliding the  
106 semilandmarks by minimising procrustes distance rather than bending  
107 energy (REFS). We used these Procrustes-aligned coordinates of all species  
108 (n=43) to calculate average shape values for each species which we then  
109 used for a principal components (PC) analysis (REFS) with the  
110 plotTangentSpace function (Adams et al., 2013).

## 111 **Phylogeny**

112 Instead of basing our analyses on individual trees and assuming that their  
113 topologies were known without error (e.g. Ruta et al., 2013; Foth et al.,

114 2012; Brusatte et al., 2008; Harmon et al., 2003) we used a distribution of  
115 101 pruned phylogenies derived from the randomly resolved mammalian  
116 supertrees in (Kuhn et al., 2011).

117 Eight species (six *Microgale* tenrecs and two golden moles) in our  
118 morphological data were not in the phylogenies. Phylogenetic  
119 relationships among the *Microgale* have not been resolved more recently  
120 than the (Kuhn et al., 2011) analysis, therefore we added the additional  
121 *Microgale* species at random to the *Microgale* genus within each phylogeny  
122 (Revell, 2012). We could not use the same approach to add the two  
123 missing golden mole species because they were the only representatives of  
124 their respective genera within our data. Therefore we randomly added  
125 these species to the common ancestral node (using the findMRCA function  
126 in phytools (Revell, 2012)) of all golden moles within each phylogeny.  
127 Adding these extra species to the phylogenies created polytomies which  
128 we resolved arbitrarily using zero-length branches (Paradis et al., 2004).  
129 We calculated pairwise phylogenetic distances among species using the  
130 cophenetic function (R Development Core Team, 2013).

## 131 **Analyses**

### 132 **Disparity calculations**

133 We calculated morphological disparity separately for golden moles and  
134 tenrecs in each of the morphological datasets. We used the PC axes which  
135 accounted for 95% of the cumulative variation to calculate four disparity  
136 metrics; the sum and product of the range and variance of morphospace  
137 occupied by each family (Brusatte et al., 2008; Foth et al., 2012; Ruta et al.,

2013). We also calculated morphological disparity directly from the Procrustes-superimposed shape data (Zelditch et al., 2012). Disparity is expected to be higher in larger groups (REFS). Therefore we repeated our disparity comparisons between the two families using rarefaction (see supplementary material) to confirm that observed differences in disparity between the two groups were not artefacts of differences in sample size.

To test whether tenrecs are more morphologically disparate than expected by chance, we simulated shape evolution (Harmon et al., 2008) of the species-average, Procrustes-superimposed shape coordinates of each tenrec species across our distribution of phylogenies under a Brownian Motion (BM) model (1000 simulations on each of 101 phylogenies pruned to include tenrec species only). We ran a principal components analysis on each of the simulations and used the PC axes which accounted for 95% of the cumulative variation to calculate disparity metrics.

We compared the observed disparity measure to the corresponding distribution of values and used a two-tailed test to determine whether the observed (true) disparity measures were more or less than expected by chance.

The majority of tenrecs (19 out of 31 in our data) are members of the *Microgale* (shrew-like) genus which is notable for its relatively low phenotypic diversity (Soarimalala & Goodman, 2011; Jenkins, 2003) and may mask signals of high disparity among other tenrecs. To test this we repeated our simulations of shape evolution excluding *Microgale* species. This reduced our data set for tenrecs from 31 to 12 species.

To test whether tenrecs have significantly different morphologies than golden moles, we used a non parametric MANOVA (Anderson, 2001) to



164 compare morphospace occupation between the two groups (REFS?).

## 165 **Results**

### 166 **Morphological disparity in tenrecs**

167 We compared observed disparity to the distributions of expected disparity  
168 calculated from BM simulations of shape data (1,000 simulations on each  
169 of 101 phylogenies). We present the results from comparing our observed  
170 and simulated measures of sum of variance (figures 3 and y) because all  
171 disparity metrics yielded the same patterns: tenrecs have significantly  
172 lower disparity than expected by chance. Full results from all disparity  
173 metrics and including the ventral and lateral skull views can be found in  
174 the supplementary.

175 Removing the phenotypically similar *Microgale* tenrecs did not  
176 qualitatively affect our results; the non-*Microgale* tenrecs still show  
177 significantly lower phenotypic disparity than expected by chance  
178 (simulation results in the supplementary material).

### 179 **Morphological disparity in tenrec and golden moles**

180 Figures 5 and 6 depict the morphospace plots derived from our principal  
181 components analyses of average Procrustes-superimposed shape  
182 coordinates for each species in our skull and mandible data respectively.  
183 We used the principal components axes which accounted for 95% of the  
184 cumulative variation ( $n = 6$  axes for the dorsal skulls analysis and  $n = 11$   
185 axes for the mandibles) to calculate the disparity of each family.

186 There was agreement among all of our disparity metrics that tenrecs  
187 have more diverse dorsal skull shapes than golden moles and the two  
188 families occupy significantly different areas of morphospace  
189 (npMANOVA,  $F = 59.34$ ,  $R^2 = 0.59$ ,  $p = 0.001$ ).

190 Unexpectedly, our analyses of disparity in mandible shape yielded the  
191 opposite result; golden moles have higher disparity in the shape of their  
192 mandibles than tenrecs and they occupy significantly different areas of  
193 morphospace (npMANOVA  $F = 59.34$ ,  $R^2 = 0.59$ ,  $p = 0.001$ )

194 However, this result may be an artefact of the relatively low phenotypic  
195 diversity within *Microgale* tenrecs. Golden moles and non-*Microgale*  
196 tenrecs occupy significantly different areas of morphospace (npMANOVA  
197  $F = 31.6$ ,  $R^2 = 0.59$ ,  $p = 0.001$ ). However, the overall differences in  
198 morphospace occupation are only supported by some of the disparity  
199 metrics. When disparity is calculated as the product of variance or  
200 product of ranges, golden moles have higher disparity than non-*Microgale*.  
201 In contrast, there is no significant difference between the two groups  
202 when disparity is measured as the sum of ranges or the sum of variance.

## 203 Discussion

204 Our findings provide new insights into phenotypic diversity within the  
205 tenrec family. Contrary to previous suggestions (e.g. Eisenberg & Gould,  
206 1969; Olson, 2013), tenrecs do not appear to be exceptional in their  
207 morphological diversity. They do seem to be more morphologically  
208 disparate than their closest relatives but only in skull morphology; the  
209 opposite is true when we look at mandible morphology (figure 6). Our

210 results illustrate the vital importance of applying quantitative methods to  
211 test assumptions about morphological diversity.

212 Tenrecs are evidently a diverse group, both phenotypically and  
213 ecologically. Body sizes of extant tenrecs span three orders of magnitude  
214 (2.5 to >2,000g) which is a greater range than all other Families, and most  
215 Orders, of living mammals (Olson & Goodman, 2003). Within this vast  
216 size range there is striking morphological diversity, from the spiny  
217 *Echinops*, *Setifer* and striking *Hemicentetes* to the shrew-like *Microgale*.  
218 Furthermore, tenrecs inhabit a variety of ecological niches and habitats  
219 including terrestrial, arboreal, semi-aquatic and semi-fossorial forms  
220 (REFS).

221 However, our results cast doubt over whether the evident diversity  
222 within the tenrec family should be considered to be an adaptive radiation.  
223 Phenotypic and ecological divergences within a clade are not surprising;  
224 most clades have at least small levels of disparity so, when it comes to  
225 identifying adaptive radiations, it's important to identify clades which are  
226 exceptional in their diversity (Losos & Mahler, 2010). Here we have  
227 presented the first quantitative investigation of morphological disparity in  
228 tenrecs and our results suggest that perhaps phenotypic variation in  
229 tenrecs is not the product of an adaptive radiation in the strict sense of its  
230 definition.

231 Although tenrecs are not more morphologically diverse than expected  
232 by chance, they do show greater cranial disparity than their nearest  
233 relatives. The discrepancies between our analyses of cranial and mandible  
234 disparity could reflect derive from factors associated with the modularity  
235 of morphological evolution.

236 There is strong evidence that morphological variation in skulls and  
237 mandibles is derived from differential evolution of integrated  
238 developmental modules (reviewed by Klingenberg, 2013). For example,  
239 there seems to be two primary modules in the mouse mandible; an  
240 alveolar part which holds the teeth and the ascending ramus for muscle  
241 attachment and which articulates with the skull (Klingenberg, 2008).  
242 Geometric shape covariation is stronger within rather than between these  
243 modules.

244 Our landmarks and curves for the mandibles (figure 2, table 2) include  
245 aspects of variation in the dentition but they focus particular attention on  
246 the ascending ramus (condyloid, condylar and angular processes).  
247 Therefore the higher morphological disparity in golden mole mandibles  
248 most likely reflects greater variation in the shape of the muscle attachment  
249 areas of the mandible. In contrast it proved impossible to position reliable  
250 landmarks on the corresponding articulation areas of the skull in lateral  
251 view (see supplementary).

252 If variation in muscle attachment/articulation sites is driving  
253 morphological disparity in mandibles, it is not clear why golden moles  
254 should have more disparate articular rami than tenrecs.

255 While our findings cast doubt on the designation of tenrecs as an  
256 adaptive radiation sensu (Losos & Mahler, 2010), there are certain caveats  
257 to consider which could modify the interpretation of our results.

258 Phenotypic variation can evolve for reasons other than adaptive  
259 radiation. Therefore, to describe phenotypic divergence as the product of  
260 an adaptive radiations requires exceptional morphological diversity in  
261 traits which have specific and proven adaptive significance (Losos &

262 Mahler, 2010). The evolution of cranial shape (both upper skull and  
263 mandible), particularly dental morphology, has obvious correlations with  
264 dietary specialisations (REFS) and occupation of specific ecological niches  
265 (REFS).

266 Considering the wide ecological diversity of our study species; the  
267 fossorial golden moles and semi-fossorial, arboreal, terrestrial and  
268 semi-aquatic tenrecs (REFS) it is reasonable to expect that variation in  
269 cranial shape should be an adaptive characteristic which allows the  
270 animals to survive in their divergent niches. Therefore quantifying the  
271 diversity of cranial morphology is a reasonable method of assessing the  
272 significance of morphological variety within the context of identifying an  
273 adaptive radiation.

274 Cranial shape similarities are commonly used to delineate species  
275 boundaries (REFS) or for cross-taxonomic comparative studies of  
276 phenotypic (dis)similarities (REFS). However, disparity studies are  
277 inevitably constrained to be measures of diversity within specific traits  
278 rather than overall morphology (Roy & Foote, 1997). Therefore it is  
279 possible that other morphological proxies of phenotype; analyses of linear  
280 measurements and/or discrete characters of either cranial or post-cranial  
281 morphologies could yield different results.

282 However, the results of (Foth et al., 2012) are encouraging. In an  
283 analysis of morphological disparity in pterosaurs, they found that  
284 disparity calculations based on geometric morphometric characterisation  
285 of skull shape yielded broadly similar results compared to analyses of  
286 whole-skeleton discrete characters and limb proportion data sets.  
287 Therefore the disparity patterns we find here based on geometric

288 morphometric analyses of cranial shape most likely represent  
289 approximations of disparity which are accurate for morphological  
290 diversity in the clades.

## 291 **Acknowledgements**

292 We thank the members of NERD club for insightful discussions and the  
293 museum staff and curators for their support and access to collections.  
294 Funding was provided by an Irish Research Council EMBARK Initiative  
295 Postgraduate Scholarship (SF) and the European Commission CORDIS  
296 Seventh Framework Programme (FP7) Marie Curie CIG grant. Proposal  
297 number: 321696 (NC, SF)

## 298 **References**

- 299 Adams, D., Otárola-Castillo, E. & Paradis, E. 2013. geomorph: an R  
300 package for the collection and analysis of geometric morphometric  
301 shape data. *Methods in Ecology and Evolution* **4**: 393–399.  
302 10.1111/2041-210X.12035.
- 303 Anderson, M. 2001. A new method for non-parametric multivariate  
304 analysis of variance. *Austral Ecology* **26**: 32–46.  
305 10.1111/j.1442-9993.2001.01070.pp.x.
- 306 Asher, R. & Hofreiter, M. 2006. Tenrec phylogeny and the noninvasive  
307 extraction of nuclear DNA. *Systematic Biology* **55**: 181–194.
- 308 Asher, R.J., Maree, S., Bronner, G., Bennett, N., Bloomer, P., Czechowski,  
309 P., Meyer, M. & Hofreiter, M. 2010. A phylogenetic estimate for golden

- 310 moles (Mammalia, Afrotheria, Chrysochloridae). *BMC Evolutionary*  
311 *Biology* **10**: 1–13.
- 312 Brusatte, S., Benton, M., Ruta, M. & Lloyd, G. 2008. Superiority,  
313 competition and opportunism in the evolutionary radiation of  
314 dinosaurs. *Science* **321**: 1485–1488.
- 315 Eisenberg, J.F. & Gould, E. 1969. The Tenrecs: A Study in Mammalian  
316 Behaviour and Evolution. *Smithsonian Contributions to Zoology* **27**: 1–152.
- 317 Erwin, D. 2007. Disparity: morphological pattern and developmental  
318 context. *Palaeontology* **50**: 57–73.
- 319 Foote, M. 1997. The evolution of morphological diversity. *Annual Review of*  
320 *Ecology and Systematics* **28**: 129–152.
- 321 Foth, C., Brusatte, S. & Butler, R. 2012. Do different disparity proxies  
322 converge on a common signal? Insights from the cranial morphometrics  
323 and evolutionary history of *Pterosauria* (Diapsida: Archosauria). *Journal*  
324 *of Evolutionary Biology* **25**: 904–915. 10.1111/j.1420-9101.2012.02479.x.
- 325 Gavrillets, S. & Losos, J. 2009. Adaptive radiation: contrasting theory with  
326 data. *Science* **323**: 732–736. 10.1126/science.1157966.
- 327 Goswami, A., Milne, N. & Wroe, S. 2011. Biting through constraints:  
328 cranial morphology, disparity and convergence across living and fossil  
329 carnivorous mammals. *Proceedings of the Royal Society B: Biological*  
330 *Sciences* **278**: 1831–1839. 10.1098/rspb.2010.2031.
- 331 Harmon, L., Schulte, J., Larson, A. & Losos, J.B. 2003. Tempo and mode of  
332 evolutionary radiation in iguanian lizards. *Science* **301**: 961–964.

- 333 Harmon, L., Weir, J., Brock, C., Glor, R. & Challenger, W. 2008. GEIGER:  
334 investigating evolutionary radiations. *Bioinformatics* **24**: 129–131.
- 335 Hopkins, M. 2013. Decoupling of taxonomic diversity and morphological  
336 disparity during decline of the Cambrian trilobite family *Pterocephaliidae*.  
337 *Journal of Evolutionary Biology* **26**: 1665–1676. 10.1111/jeb.12164.
- 338 IUCN 2012. International Union for Conservation of Nature.
- 339 Jenkins, P. 2003. *Microgale, shrew tenrecs*, pp. 1273–1278. The University of  
340 Chicago Press, Chicago.
- 341 Klingenberg, C. 2008. Morphological integration and developmental  
342 modularity. *Annual review of ecology, evolution, and systematics* **39**:  
343 115–132.
- 344 Klingenberg, C. 2013. Cranial integration and modularity: insights into  
345 evolution and development from morphometric data. *Hystrix, the Italian*  
346 *Journal of Mammalogy* **24**: 43–58.
- 347 Kuhn, T., Mooers, A. & Thomas, G. 2011. A simple polytomy resolver for  
348 dated phylogenies. *Methods in Ecology and Evolution* **2**: 427–436.  
349 10.1111/j.2041-210X.2011.00103.x.
- 350 Losos, J. 2010. Adaptive radiation, ecological opportunity, and  
351 evolutionary determinism. American Society of Naturalists E. O. Wilson  
352 Award Address. *The American Naturalist* **175**: 623–639. 10.1086/652433.
- 353 Losos, J.B. & Mahler, D. 2010. *Adaptive radiation: the interaction of ecological*  
354 *opportunity, adaptation and speciation*, chap. 15, pp. 381–420. Sinauer  
355 Association, Sunderland, MA.



- 356 MacLeod, N. 2013. Landmarks and semilandmarks: Difference without  
357 meaning and meaning without difference.
- 358 Olson, L. & Goodman, S. 2003. *Phylogeny and biogeography of tenrecs*, pp.  
359 1235–1242. The University of Chicago Press, Chicago.
- 360 Olson, L.E. 2013. Tenrecs. *Current Biology* **23**: R5–R8.
- 361 O'Meara, B., Ané, C., Sanderson, M. & Wainwright, P. 2006. Testing for  
362 different rates of continuous trait evolution using likelihood. *Evolution*  
363 **60**: 922–933. 10.1111/j.0014-3820.2006.tb01171.x.
- 364 Paradis, E., Claude, J. & Strimmer, K. 2004. Ape: Analyses of  
365 Phylogenetics and Evolution in R language. *Bioinformatics* **20**: 289–290.  
366 10.1093/bioinformatics/btg412.
- 367 Price, S., Tavera, J., Near, T. & Wainwright, P. 2013. Elevated rates of  
368 morphological and functional diversification in reef-dwelling haemulid  
369 fishes. *Evolution* **67**: 417–428. 10.1111/j.1558-5646.2012.01773.x.
- 370 Revell, L. 2012. phytools: an R package for phylogenetic comparative  
371 biology (and other things). *Methods in Ecology and Evolution* **3**: 217–223.
- 372 Rohlf, F. 2012. Tpsutil.
- 373 Rohlf, F. 2013. Tpsdig2 ver 2.17.
- 374 Rohlf, J. & Marcus, L. 1993. A revolution in morphometrics. *Trends in*  
375 *Ecology & Evolution* **8**: 129–132.
- 376 Roy, K. & Foote, M. 1997. Morphological approaches to measuring  
377 biodiversity. *Trends in Ecology & Evolution* **12**: 277–281.

- 378 Ruta, M., Angielczyk, K., Fröbisch, J. & Benton, M. 2013. Decoupling of  
379 morphological disparity and taxic diversity during the adaptive  
380 radiation of anomodont therapsids. *Proceedings of the Royal Society B:*  
381 *Biological Sciences* **280**: 20131071. 10.1098/rspb.2013.1071.
- 382 Soarimalala, V. & Goodman, S. 2011. *Les petits mammifères de Madagascar*.  
383 Guides sur la diversité biologique de Madagascar. Association Vahatra,  
384 Antananarivo, Madagascar.
- 385 Team, R.D.C. 2013. R: A language and environment for statistical  
386 computing.
- 387 Wilson, D. & Reeder, D. 2005. *Mammal species of the world. A taxonomic and*  
388 *geographic reference (3rd ed)*. Johns Hopkins University Press.
- 389 Zelditch, M., Swiderski, D. & Sheets, D. 2012. *Geometric Morphometrics for*  
390 *Biologists, second edition*. Academic Press, Elsevier, United States of  
391 America.

## List of Figures

393	1	Landmarks (red points) and curves (blue lines) used to capture the morphological shape of skulls in dorsal view. Curves were re-sampled to the same number of evenly-spaced points. See table X for description of curves and landmarks.	
394		<i>Potamogale</i>	
395		<i>velox</i> (Tenrecidae) skull, accession number: AMNH_51327 . . .	20
396			
397			
398	2	Landmarks (red points) and curves (blue lines) used to capture the morphological shape of mandibles. Curves were re-sampled to the same number of evenly-spaced points. See table X for description of curves and landmarks.	
399		<i>Potamogale</i>	
400		<i>velox</i> (Tenrecidae) mandible, accession number: AMNH_51327	21
401			
402			
403	3	Comparison of the observed and expected disparity in the dorsal skulls. Disparity is measured as sum of variance, blue arrow points to the observed value of disparity (0.0017) . . .	22
404			
405			
406	4	Comparison of the observed and expected disparity in the mandibles. Disparity is measured as sum of variance, blue arrow points to the observed value of disparity (0.0031) . . .	23
407			
408			
409	5	Principal components plot of the dorsal skulls' morphospace occupied by tenrecs (red, n=31) and golden moles (black, n=12). Axes are PC1 and PC2 of the average scores from a PCA analysis of mean Procrustes shape coordinates for each species. . . . .	24
410			
411			
412			
413			
414	6	Principal components plot of the mandibles' morphospace occupied by tenrecs (red, n=31) and golden moles (black, n=12). Axes are PC1 and PC2 of the average scores from a PCA analysis of mean Procrustes shape coordinates for each species.	
415			
416			
417			
418		25	

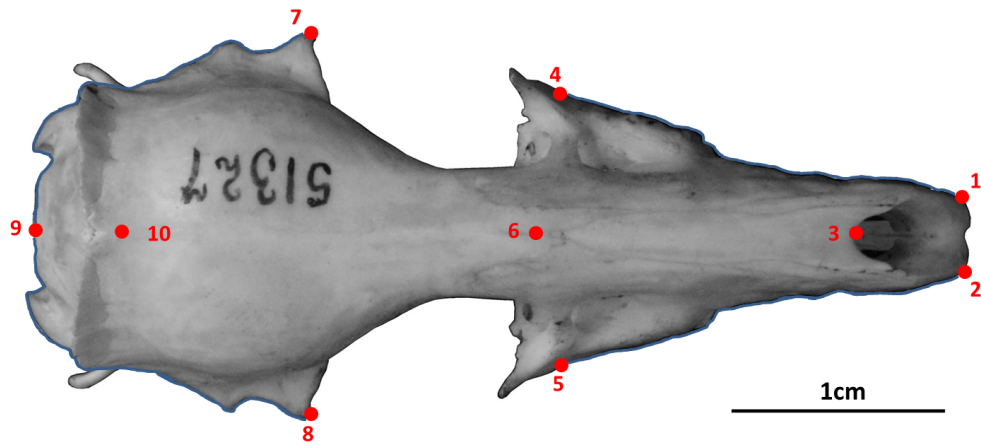


Figure 1: Landmarks (red points) and curves (blue lines) used to capture the morphological shape of skulls in dorsal view. Curves were re-sampled to the same number of evenly-spaced points. See table X for description of curves and landmarks. *Potamogale velox* (Tenrecidae) skull, accession number: AMNH\_51327

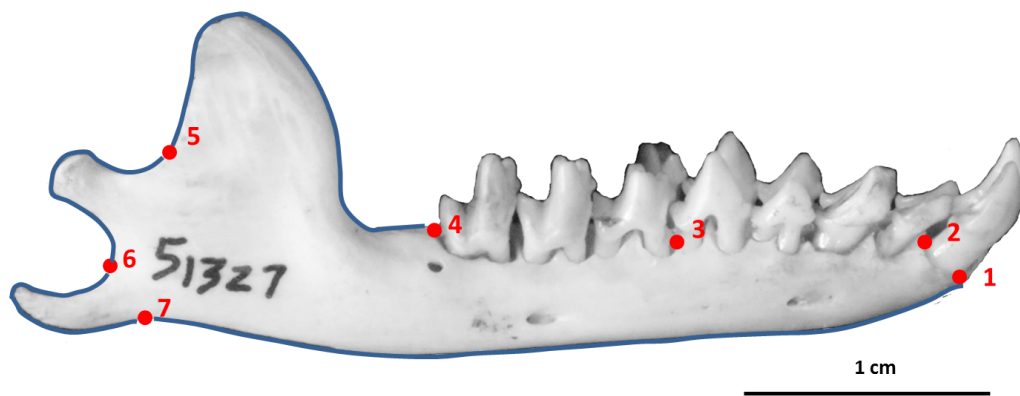


Figure 2: Landmarks (red points) and curves (blue lines) used to capture the morphological shape of mandibles. Curves were re-sampled to the same number of evenly-spaced points. See table X for description of curves and landmarks. *Potamogale velox* (Tenrecidae) mandible, accession number: AMNH\_51327

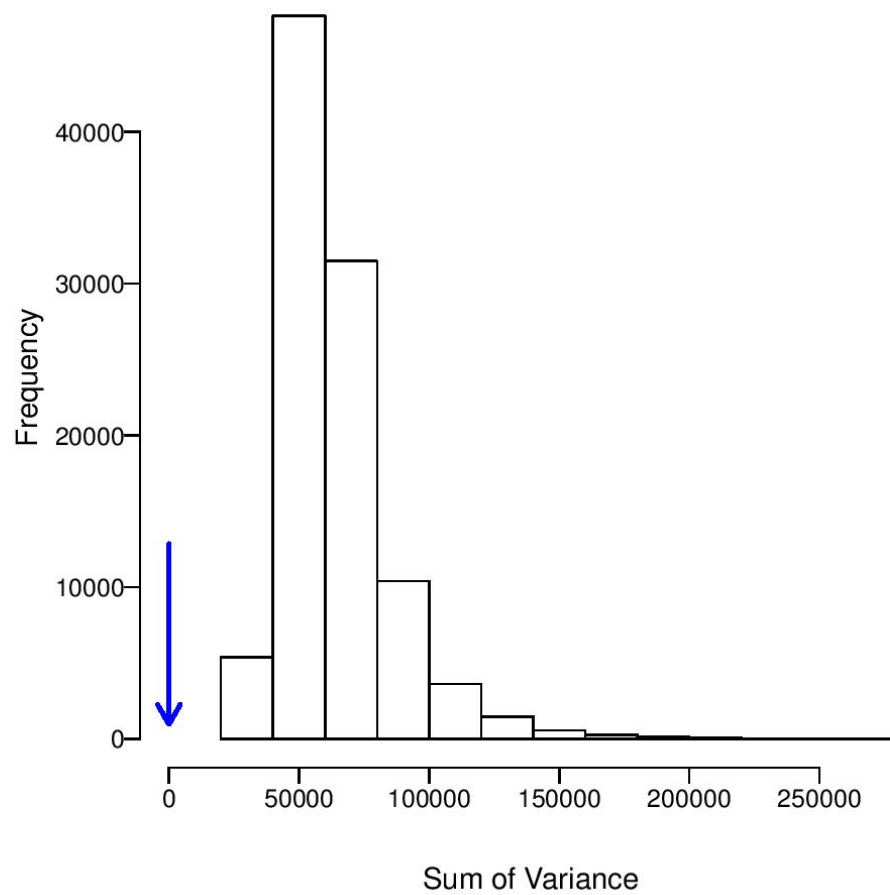


Figure 3: Comparison of the observed and expected disparity in the dorsal skulls. Disparity is measured as sum of variance, blue arrow points to the observed value of disparity (0.0017)

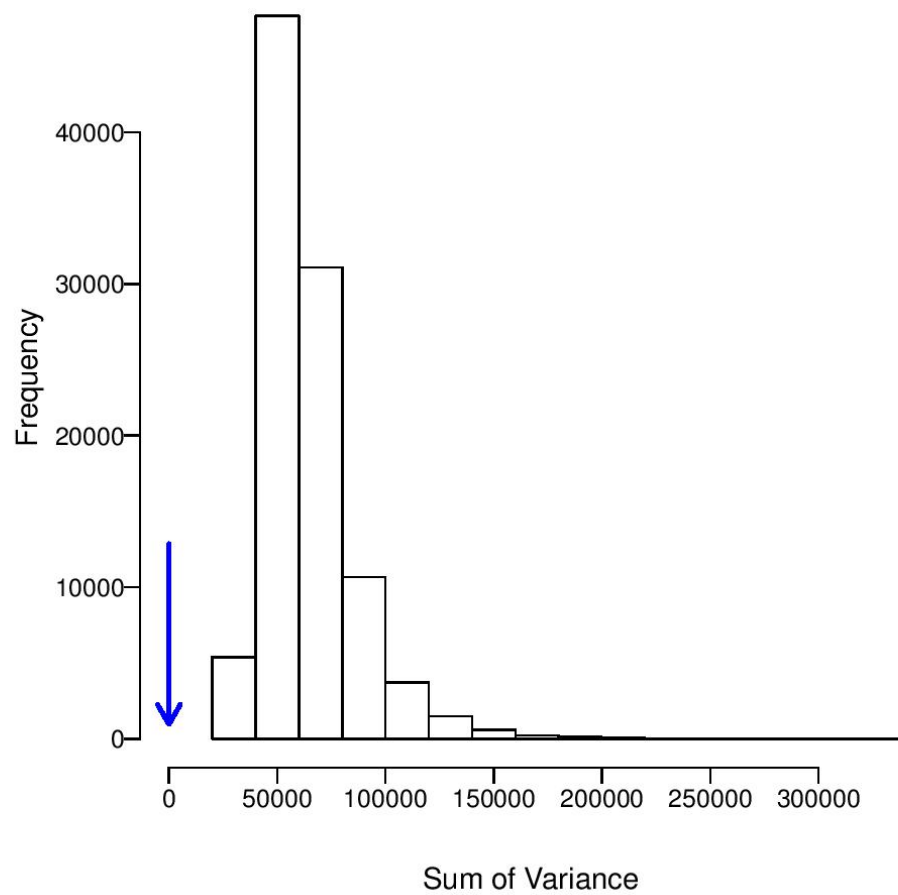


Figure 4: Comparison of the observed and expected disparity in the mandibles. Disparity is measured as sum of variance, blue arrow points to the observed value of disparity (0.0031)

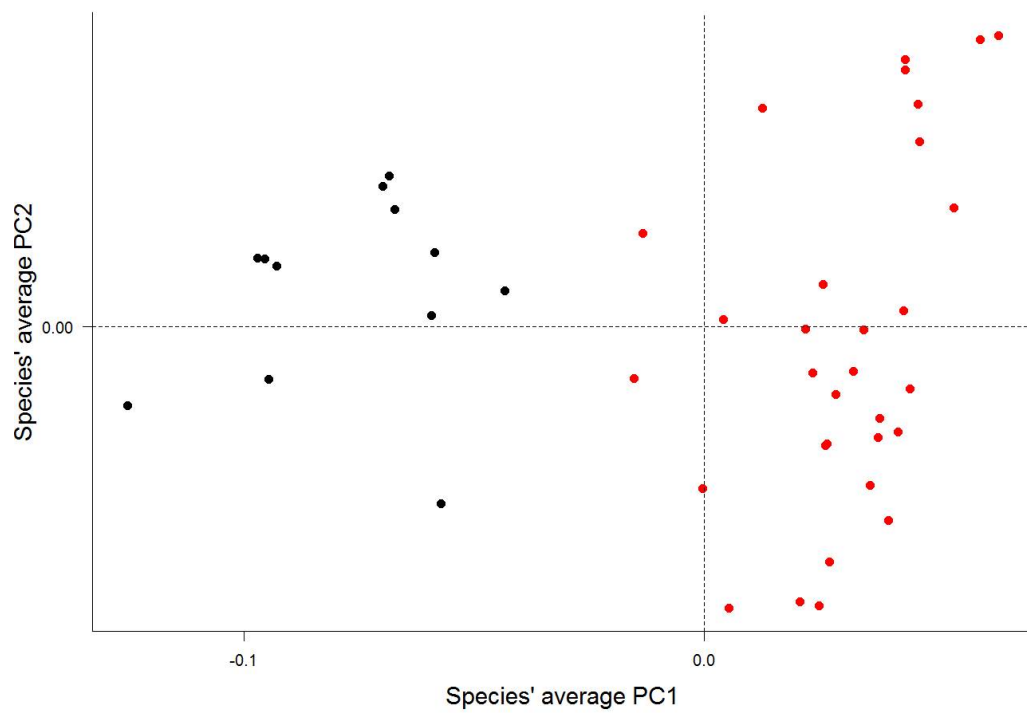


Figure 5: Principal components plot of the dorsal skulls' morphospace occupied by tenrecs (red,  $n=31$ ) and golden moles (black,  $n=12$ ). Axes are PC1 and PC2 of the average scores from a PCA analysis of mean Procrustes shape coordinates for each species.



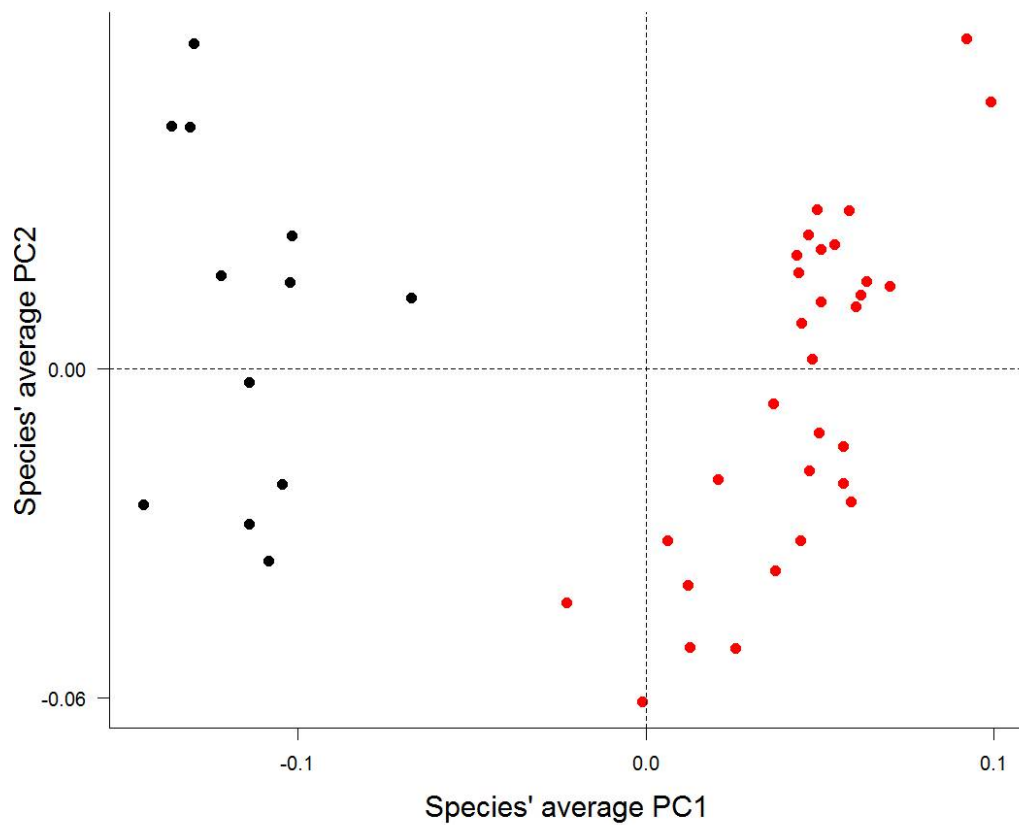


Figure 6: Principal components plot of the mandibles' morphospace occupied by tenrecs (red,  $n=31$ ) and golden moles (black,  $n=12$ ). Axes are PC1 and PC2 of the average scores from a PCA analysis of mean Procrustes shape coordinates for each species.

## 419 List of Tables

420	1	Descriptions of the landmarks (points) and curves (semi-	
421		landmarks) for the skulls in dorsal view (see Figure 1). . . . .	27
422	2	Descriptions of the landmarks (points) and curves (semi-	
423		landmarks) for the mandibles in lateral (buccal) view (see	
424		figure 2) . . . . .	28
425	3	Comparison of observed and simulated disparity measures	
426		for the dorsal skulls analysis; observed (true) disparity mea-	
427		sures, minimum simulated value (sim.min), maximum sim-	
428		ulated value (sim.max), standard deviation of the simulated	
429		values (sdev.sim) and p value comparing the observed dis-	
430		parity measures to the distribution of simulated values) . . .	29
431	4	Comparison of observed and simulated disparity measures	
432		for the mandibles analysis; observed (true) disparity mea-	
433		sures, minimum simulated value (sim.min), maximum sim-	
434		ulated value (sim.max), standard deviation of the simulated	
435		values (sdev.sim) and p value comparing the observed dis-	
436		parity measures to the distribution of simulated values) . . .	30

Table 1: Descriptions of the landmarks (points) and curves (semilandmarks) for the skulls in dorsal view (see Figure 1).

Landmark	Description
1 + 2	Left (1) and right (2) anterior points of the premaxilla
3	Anterior of the nasal bones in the midline
4 + 5	Maximum width of the palate (maxillary) on the left (4) and right (5)
6	Midline intersection between nasal and frontal bones
7 + 8	Widest point of the skull on the left (7) and right (8)
9	Posterior of the skull in the midline
10	Posterior intersection between saggital and parietal sutures
<b>Curve A</b> (12 points)	Outline of the braincase on the left side, between landmarks 9 and 7 (does not include visible features from the lower (ventral) side of the skull)
<b>Curve B</b> (10 points)	Outline of the palate on the left side, between landamarks 4 and 1 (outline of the rostrum only, not the shape of the teeth)
<b>Curve C</b> (12 points)	Outline of the braincase on the right side, between landmarks 9 and 8 (does not include visible features from the lower (ventral) side of the skull)
<b>Curve D</b> (10 points)	Outline of the palate on the right side, between landamarks 5 and 2 (outline of the rostrum only, not the shape of the teeth)

Table 2: Descriptions of the landmarks (points) and curves (semilandmarks) for the mandibles in lateral (buccal) view (see figure 2)

Landmark	Description
1	Anterior of the alveolus of the first incisor
2	Posterior of the alveolus of the first incisor
3	Anterior of the alveolus of the first molar
4	Posterior of the alveolus of the last molar
5	Maximum curvature between the coronoid and condylar processes
6	Maximum curvature between the condylar and angular processes
7	Maximum curvature between the angular process and the horizontal ramus
Curve A	Condylar process (between landmarks 4 and 5, 15 points)
Curve B	Condylar process (between landmarks 5 and 6, 15 points)
Curve C	Angular process (between landmarks 6 and 7, 15 points)
Curve D	Base of the jaw (between landmarks 7 and 1, 12 points)

Table 3: Comparison of observed and simulated disparity measures for the dorsal skulls analysis; observed (true) disparity measures, minimum simulated value (sim.min), maximum simulated value (sim.max), standard deviation of the simulated values (sdev.sim) and p value comparing the observed disparity measures to the distribution of simulated values)

<b>Disparity metric</b>	<b>Observed</b>	<b>Sim.min</b>	<b>Sim.max</b>	<b>Sdev.sim</b>	<b>p value</b>
Sum of Variance	0.0017	25067.35	278042.5	21384.02	0
Product of Variance	0.00011	1154.63	52705.84	1636.32	0
Sum of Ranges	0.41	1521.15	3007.42	168.03	0
Product of Ranges	0.043	142.94	881.3	46.04	0
ZelditchMD	0.0018	31289.41	416863.5	27062.58	0

Table 4: Comparison of observed and simulated disparity measures for the mandibles analysis; observed (true) disparity measures, minimum simulated value (sim.min), maximum simulated value (sim.max), standard deviation of the simulated values (sdev.sim) and p value comparing the observed disparity measures to the distribution of simulated values)

<b>Disparity metric</b>	<b>Observed</b>	<b>Sim.min</b>	<b>Sim.max</b>	<b>Sdev.sim</b>	<b>p value</b>
Sum of Variance	0.0033	23128.23	334094.4	21417.05	0
Product of Variance	0.00016	1093.05	56893.42	1660.66	0
Sum of Ranges	0.7	135.5306	926.47	46.24	0
Product of Ranges	0.003	29503.47	390453.2	27070.41	0